

## Performance analyzes of a compact Pico hydropower plant with a wide operating range

Pudji Irasari<sup>1</sup>, Anwar Muqorobin<sup>1</sup>, Puji Widiyanto<sup>1</sup>, Tajuddin Nur<sup>2</sup>, I Nengah Diasta<sup>3</sup>,  
Priyono Sutikno<sup>3</sup>

<sup>1</sup>Research Center for Energy Conversion and Conservation, National Research and Innovation Agency, Bandung, Indonesia

<sup>2</sup>Department of Electrical Engineering, Atma Jaya Catholic University of Indonesia, Jakarta, Indonesia

<sup>3</sup>Research Center for New and Renewable Energy, Bandung Institute of Technology, Bandung, Indonesia

### Article Info

#### Article history:

Received Mar 4, 2022

Revised Sep 7, 2022

Accepted Sep 23, 2022

#### Keywords:

Performance characteristics  
Permanent magnet generator  
Pico hydropower plant  
Power converter  
THDv

### ABSTRACT

This paper analyzes the performance of a Pico hydropower plant consisting of an axial hydro turbine integrated with a permanent magnet generator (PMG) and connected to a power converter. The proposed system is aimed to obtain a wide system operation range to gain more power captured while maintaining time-harmonic distortion in voltage (THDv) that meets the standard. The PMG specification is 1 kW, 1 phase, 235 V, 50 Hz, 83 rpm. The design and simulation of PMG were carried out by analytical and numerical calculations using FEMM 4.2. The power converter was simulated using PSIM and functions to reduce the THDv and pass the generator voltage between 50–500 V. The results show the THDv of the generating system at the upper and lower limits of the passed voltage having a THDv below 5%. Meanwhile, the PMG performance characteristics at various currents and rotations produce efficiency of 87.20% at nominal current. From these results, it can be concluded that the Pico hydropower plant works well as desired.

This is an open access article under the [CC BY-SA](https://creativecommons.org/licenses/by-sa/4.0/) license.



### Corresponding Author:

Pudji Irasari

Research Center for Energy Conversion and Conservation, National Research and Innovation Agency  
Cisitu St, Komplek BRIN, Bandung 40135, Indonesia

Email: pudj003@brin.go.id

## 1. INTRODUCTION

Very-low head Pico hydropower (VLHPHP) has been increasingly developed in the last decade. This plant provides an opportunity to explore hydro energy from stream rivers with large discharges and very-low heads that mostly flow through urban or agricultural areas. VLHPHP does not require piping and dams to be built along the river and close to the load [1]. Its easy-to-reach location makes it easy to monitor, operate, and maintain. In addition, VLHPHP can be integrated with existing sluice gates to save construction costs.

A Pico hydro is defined with different capacities, namely <10 kW [2] and <5 kW [3], while a very-low head is a less than 3 m head [1]. Studies related to VLHPHP with a power of <5 kW are being focused on the main components, namely the very-low head Pico hydro turbine [4]–[7], generator [8], [9], power controller [10]–[12], as well as a combination of two or all of these components [13]–[16]. Due to relatively small power, VLHPHP is more efficient without mechanical transmission and using a multi-pole generator. The type of generator used is generally asynchronous or permanent magnet generator (PMG). However, lately, PMG has become increasingly popular because of its advantages over asynchronous generators, such as higher efficiency and compact construction [11], [17].

The study of the Pico hydro system done by [13] has conducted some experiments to obtain the axial hydro turbine-PMG set characteristics. The generator was designed to produce 2 kW, 3×350 V at 750 rpm. Another study showed that a Pico hydro system test consisting of a supply pipe, dual-blades reaction turbine, AC generator, and a monitoring system was carried out by Palanisamy and Thirunavukarasu [14]. The results exhibited that the system produces 2.4 kWh/day of power. No-load testing was also conducted by Sadowski [15] on power converter-PMG using a variable prime mover with a speed of 0 – 750 rpm. The results indicate that the power converter voltage controller still needed to be improved for better voltage amplitude significantly when the water turbine rotation is changed. Saura *et al.* [16], tested a lab-scale Pico hydro system consisting of a Pelton turbine and a 9 V DC motor used as a generator to supply a 5 mm light-emitting diode. Tests were carried out by varying the blade material (plastic and aluminum), the blade numbers (2-10 pieces), and the head height (15–65 cm). The best system performance produces 5.46 output voltage, achieved at 65 cm head, 5.52 l/s of flow rate, and using 10- plastic blades.

The power electronic converter (PEC) serves as the generating system's output voltage and frequency stabilizer. In addition, PEC also reduces harmonics and controls the power factor [18]. PEC in Pico hydropower systems generally uses a dummy load and without a dummy load [19]. The control system using a dummy load requires much wiring and smooth step switching to produce reasonable control. For this reason, the dummy load capacity is the same as the generating capacity. The weakness of this system is that the two converters on the generator and load side must have the same power rating as the generator capacity [20].

The control of Pico hydropower using a dummy load connected to a 3-phase, 4 kW induction generator is carried out by Huang *et al.* [21] to make better power quality while keeping voltage and frequency at the expected degree. The dummy load was also simulated by Xu *et al.* [22] using a 3-phase, 1 kW induction generator and a 3-phase, 1 kVA synchronous generator, respectively, to investigate the impacts of harmonic distortions caused by electronic load controller installation. In comparison [10] simulates and tests an inverter for 1 kW 1-phase Pico hydro without defining the type of generator. The inverter can be used for multiple generators on a remote microgrid and lower the THDv. A power converter simulation was also carried out on Pico hydro by taking a 2.3 kW 3-phase PMG [11]. The study suggested a control algorithm employed for load balancing, harmonics diminution, and reactive power enhancement when a three-phase PMG supplies a single-phase nonlinear load. Another study discusses the design procedure for connecting Pico hydro to the grid using a power converter, where the load side used a PV inverter grid interface [12]. The generator capacity is about 1.3 kW without specifying the type.

This work analyzes the performance of a Pico hydropower plant with the proposed construction comprising an axial hydro turbine and 1-phase, 1 kW, 50 Hz, 83 rpm PMG connected with a power converter. The rotor of the PMG is integrated with that of the axial hydro turbine to get a compact system. The study aims to obtain an extensive system operation range to capture more power while maintaining time-harmonic distortion in voltage (THDv) of the system that meets the IEEE Std 519-1992. PMG characteristics are extracted at various loads and frequencies. The output voltage of the rectifier and inverter are simulated using PSIM, while analytical and numerical simulations using FEMM 4.2 are carried out to obtain the PMG characteristics.

## 2. METHOD

### 2.1. System construction and defined parameters

The compact construction of Pico hydro is represented by the unified structure of the turbine generator in Figure 1, showing the generator rotor position on the perimeter of the turbine blades. The turbine is a propeller or axial type with 24 guide vanes and 8 runner blades. Simulation at 90 rpm, head 1,329 m, and flow rate 256 kg/s, with tilt angle 45° produces turbine power of 2514.71 W [23]. Permanent magnets use the N45H type with  $B_r = 1.32$  T and  $H_b = 995$  kA/m. Several parameters are determined to obtain the electrical parameters of the generator at the nominal frequency, as tabulated in Table 1.

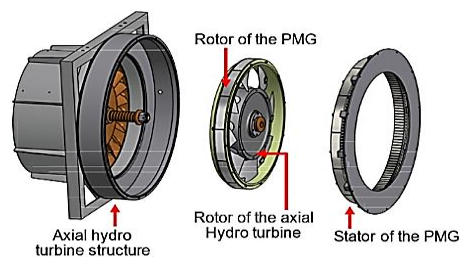


Figure 1. Axial hydro turbine-PMG assembly

Table 1. The defined parameters

Parameters, symbol	Value	Unit
Inner rotor diameter, $D_i$	0.624	m
Air gap length, $l_g$	3	mm
Rotation, $n$	83	rpm
Pole numbers, $2p$	72	poles
Nominal frequency, $f$	50	Hz
Phase number, $m$	1	phase
Current density	3.4	A/mm <sup>2</sup>

## 2.2. Electromotive force (EMF)

The instantaneous and r.m.s phase EMF generated by the magnetic flux of the permanent magnet when the rotor rotates is obtained using (1)-(3) [24].

$$E_{ph} = \frac{d\psi_M}{dt} = \omega\psi_M \sin(n\omega t + \gamma) \quad (1)$$

$$E_{ph\_rms} = \frac{1}{\sqrt{2}}\omega\psi_M = \frac{1}{\sqrt{2}}\omega k_w N_{ph} \Phi_M \quad (2)$$

$$\Phi_M = \frac{B_g D_i l_i}{p} \quad (3)$$

Where  $E_{ph}$  is the instantaneous EMF,  $E_{ph\_rms}$  is the r.m.s phase EMF,  $\gamma$  is the displacement angle between the axis of the stator winding to that of the rotor pole,  $\psi_M$  is the magnetic linkage flux,  $n$  is the harmonic order,  $\omega$  is the angular frequency,  $k_w$  is the winding factor,  $N_{ph}$  is the winding number,  $\Phi_M$  is the magnetic flux,  $B_g$  is the air gap flux density,  $l_i$  is the stator core effective length, and  $p$  is the pole pairs.

$E_{ph}$  induces stator coils having a phase resistance of  $R_1$ , the d- and q- axis synchronous reactance  $X_d$  and  $X_q$ , respectively, and producing a terminal voltage  $V_T$  of:

$$V_T = \sqrt{(E_{ph} - I_a R_1)^2 - (I_a X_q)^2 - (I_a X_d)^2} \quad (4)$$

with  $I_a$  is the armature current (A).

## 2.3. Power converter circuit

Commercial power converters transforming variable AC voltage and frequency into constant AC voltage and frequency are generally available for wind turbines but with a relatively narrow input voltage range. For example, power converter Leonics has an input voltage range of 176-265 V<sub>AC</sub> [25]. In this study, the input voltage range is more expansive to enable the system to deliver power even at a minor discharge, especially during the dry season. It is also assumed that the power system is in a rural area, so even if the power supply is small, it is still helpful for lighting. Therefore, the generator voltage passed is set between 50-500 V, and the power converter topology is shown in Figure 2.

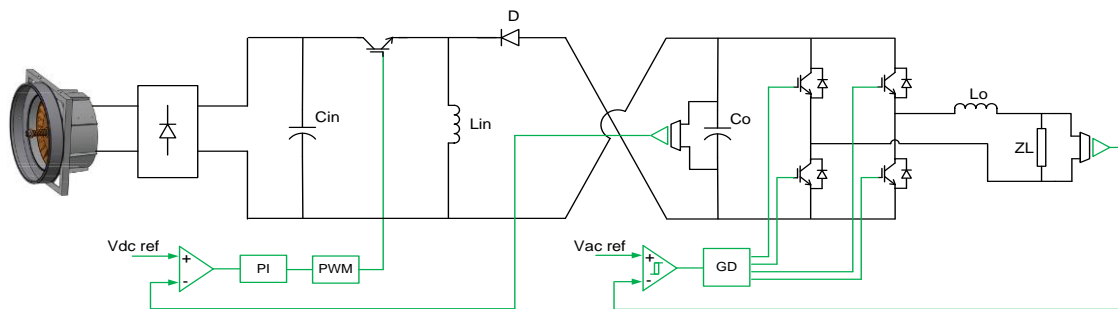


Figure 2. Axial hydro turbine-PMG connected to power converter circuit

The AC output voltage of the generator containing harmonics is rectified first to a DC voltage using a diode rectifier equipped with a capacitor. Then buck-boost converter accommodates the generator's variable voltage and produces constant DC voltage at 350 V using PI control. Furthermore, the inverter converts it to ac voltage to supply the ac load. The inductor serves to filter the output of the inverter bridge to produce a

pure sinusoidal output voltage and current. The hysteresis control with a 5 V band is employed to get the desired voltage. This control is simple to implement, has a simple structure, responds quickly, and is unaffected by changes in plant parameters. The output voltage reference is 220 Vrms, and the value of each parameter used is  $L_{in} = 5$  mH,  $C_{in} = 4700$   $\mu$ F,  $L_o = 5$  mH, and  $C_o = 470$   $\mu$ F.

#### 2.4. Losses and efficiency

When the generator rotates and is given a load of  $I_a$ , losses will arise, producing heat and reducing the output power  $P_{out}$ . These losses are due to current (copper loss  $P_{cu}$ ) and rotation (core loss  $P_{core}$  and mechanical loss  $P_{mech}$ ), respectively given by (5) and (6) [26],

$$P_{cu} = mI_a^2 R_1 \quad (5)$$

$$P_{core} = \delta_{ic} C_h f B_p^\alpha + \delta_{ic} C_e f^2 B_p^2 \quad (6)$$

where  $\delta_{ic}$  is the iron core density (kg/m<sup>3</sup>),  $C_h$  is the hysteresis loss coefficient,  $C_e$  is the eddy current loss coefficient,  $B_p$  is the peak value of magnetic flux density (T),  $\alpha$  is the constant of Steinmetz,

$$P_{mech} = P_{fric} + P_{wind} \quad (7)$$

where  $P_{fric}$  is the friction loss in bearings,  $P_{wind}$  is windage loss in the air gap.

Efficiency is obtained from

$$\eta = \frac{P_{out}}{P_{in}} \times 100\% = \frac{P_{in} - P_{cu} - P_{core} - P_{mech} - P_{add}}{mE_{ph} I_a \cos \beta} \times 100\% \quad (8)$$

where  $P_{in}$  is the input power,  $P_{add}$  is the additional loss due to leakage flux assumed as 20% of the  $P_{core}$ ,  $\cos \beta$  is the power factor = 0.9.

### 3. RESULTS AND DISCUSSION

#### 3.1. Principal dimension and nominal parameters

Figure 3 depicts the dimensions of the stator and rotor. The stator has 144 slots and  $l_i = 40$  mm as shown in Figure 3(a), while on the outer circumference of the rotor are arranged 72 permanent magnets with a per piece size of  $40 \times 20 \times 5$  mm as shown in Figure 3(b). The generator power is sourced from the magnetic flux that induces the stator coils across the air gap. Figure 4 shows the amplitude of the magnetic flux density in the air gap  $B_g$  at nominal load condition  $B_g(L)$  is lower than that of the  $B_g$  at the no-load condition  $B_g(0)$  due to demagnetization caused by the flux generated by the armature current. The difference in amplitude is 3.6%, which is generally between 1%-5% [27]. Demagnetization decreases linkage flux and ultimately reduces  $E_{ph}$ . Table 2 presents the calculating results of generator parameters at nominal frequencies. The difference between  $E_{ph}$  and  $V_T$  is 69 V is the voltage drop caused by components  $R_1$ ,  $X_d$ , and  $X_q$ .

Table 2. Nominal parameters of the generator

Parameters, symbol	Value	Unit	Parameters, symbol	Value	Unit
Winding numbers, $N_{ph}$	3312	turns	Output power, $P_{out}$	1062.12	W
Resistance, $R_1$	6.82	$\Omega$	Input power, $P_{in}$	1218.06	W
Induction voltage, $E_{ph}$	300	V	Copper loss, $P_{cu}$	138.81	W
Terminal voltage, $V_T$	231	V	Core loss, $P_{core}$	11.86	W
Armature current, $I_a$	4.51	A	Additional loss, $P_{add}$	2.37	W
d-axis sync. reactance, $X_d$	20.89	$\Omega$	Efficiency, $\eta$	87.20	%
q-axis sync. reactance, $X_q$	22.34	$\Omega$			

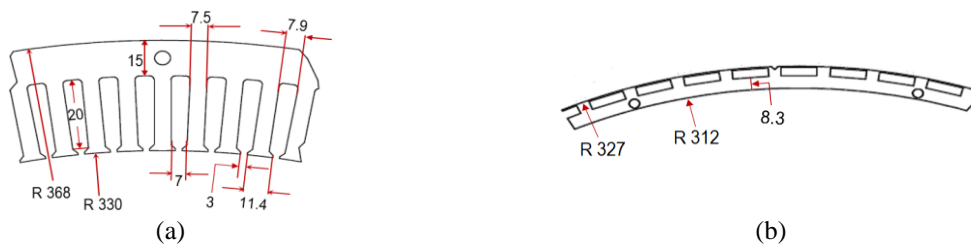


Figure 3. The dimensions of (a) stator and (b) rotor with permanent magnets, in mm unit

**3.2. Electromotive force (EMF)**

The generator voltage contains the 3rd and 5th harmonics causing voltage waves to appear at 150 Hz and 250 Hz (multiples of 3 and 5 of the base frequency), whose  $E_{ph}$  harmonic spectrum is shown in Figure 5 (a). The harmonic content distorts the fundamental  $E_{ph}$  waveform, as shown in Figure 5 (b). The maximum  $E_{ph}$  is 424.12 V at  $n = 1$  and gets higher (466.90 V) due to the 3rd and 5th harmonic content. The THDv is obtained of 23.49%, which is relatively high if the generator is directly connected to the load because, according to IEEE Std 519-1992, the maximum THDv is 5% [28]. Therefore, THDv is lowered through a filter in the power control circuit discussed in the next section.

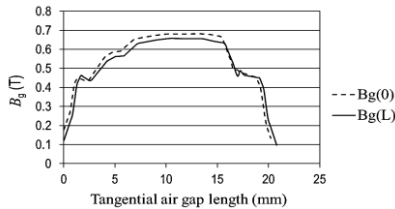


Figure 4. Air gap magnetic flux density at no-load and nominal load conditions

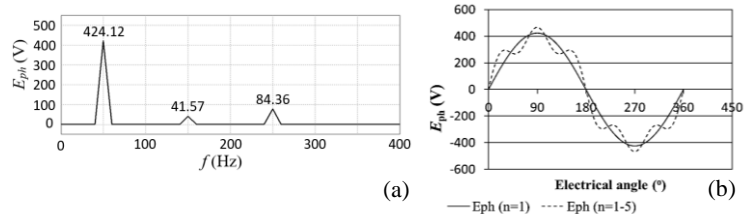


Figure 5. Harmonics on the generator voltage (a) harmonic spectrum and (b)  $E_{ph}$  waveforms at  $f = 50$  Hz

**3.3. Voltage waveform characteristics**

Figure 6 shows the simulation results of the upper limit of  $V_T$  with a maximum value of 813 V<sub>AC</sub> in Figure 6 (a) that is controlled and rectified to 350 V<sub>DC</sub> in Figure 6 (b), then converted to 220 V<sub>AC</sub>, 50 Hz with 2.2% THD in Figure 6 (c). Similarly, the simulation at the low voltage limit of 50 V in Figure 7 is carried out by controlling and rectifying the generator voltage  $V_T$  having the maximum value of 90.33 V<sub>AC</sub> shown Figure 7 (a) becomes 350 V<sub>DC</sub> in Figure 7 (b). Then the inverter converts back to an AC voltage of 220 V, 50 Hz in Figure 7 (c) with a THD of 3.63%.

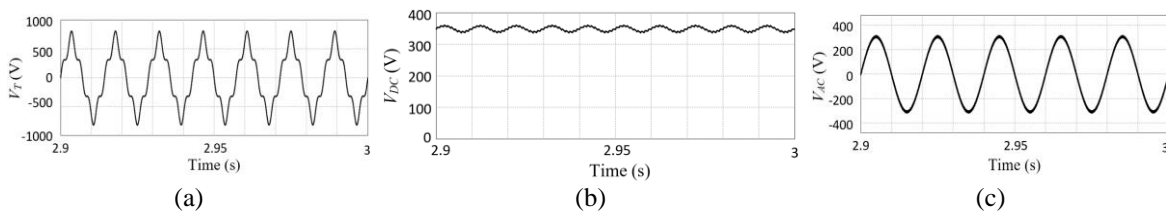


Figure 6. Simulation at high voltage limit of 500 V (a) generator, (b) rectifier, and (c) inverter

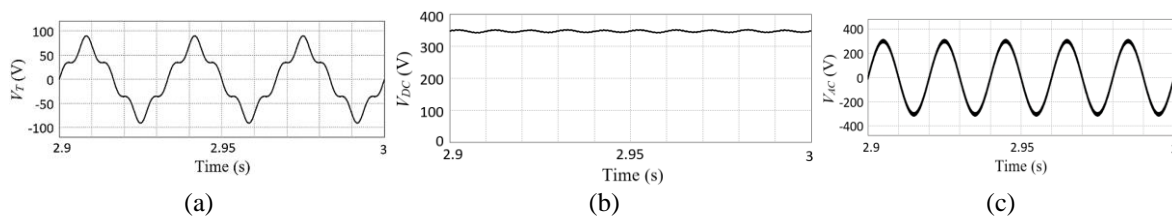


Figure 7. Simulation at low voltage limit of 50 V (a) generator, (b) rectifier, and (c) inverter

**3.4. On load characteristics**

To get the load characteristics, some of the constraints taken in the simulation are: i) the hydro energy where the Pico hydro system is installed can produce 1 kW of electrical power, ii) the maximum current is when  $V_T$  reaches the minimum value, and iii) the minimum current is set around 0.95 A. Thus, when subjected to a variable resistive load at constant rotation, the PMG produces the characteristics shown in Figure 8. The power curve at various frequencies in Figure 8(a) shows that the generator can achieve more than 1 kW of power, represented by the dotted line. At higher frequencies, the slope of the power curve becomes steeper because higher EMF is generated, resulting in a higher power at the same current. At  $f = 30$  Hz, the maximum power generated is below 1 kW, but not all can be delivered depending on the voltage generated. The steepness of the power curve decreases as the current increases due to copper loss.

Figure 8(b) shows the  $V_T$  vs.  $I_a$  curves corresponding to the power ones. At a frequency of 40–70 Hz, the dotted line is the voltage that produces power  $>1$  kW. The maximum voltage at  $f=70$  Hz is around 453 V and higher at smaller currents but still below 500 V. Meanwhile, at  $f=30$  Hz, the voltage that is not passed is  $V_T < 50$  V, which occurs at high currents due to small  $E_{ph}$  while the voltage drop is high, in this case, it happens at  $I_a > 7.52$  A.

Figure 8(c) shows the  $\eta$  vs.  $P_{out}$  curves at various frequencies with maximum efficiency for each frequency of around 93%. The higher the frequency, the smoother the efficiency curve because a high  $E_{ph}$  produces more input power, which makes it has a better resistance against the increase in losses caused by both  $I_a$  and frequency. The opposite happens at low frequencies, where the impact of the current growth is quite significant in decreasing efficiency. It can be seen at  $f=30$  Hz, exhibiting an efficiency of 69.53% at 896.76 W.

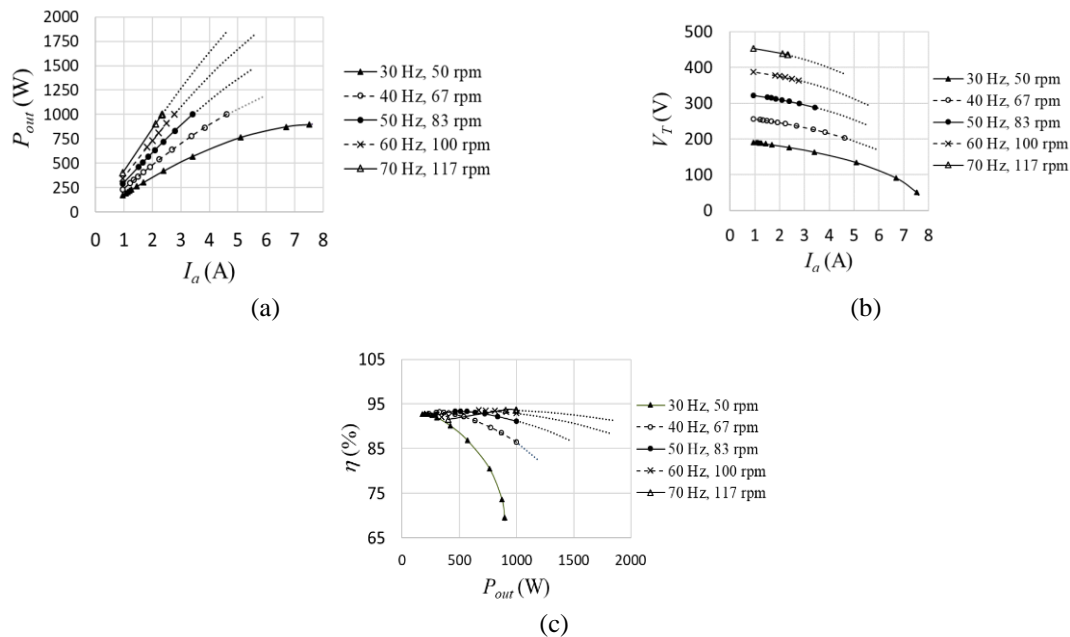


Figure 8. PMG characteristics at various frequencies, (a)  $P_{out}$  vs.  $I_a$ , (b)  $V_T$  vs.  $I_a$ , (c)  $\eta$  vs.  $P_{out}$

#### 4. CONCLUSION

This paper has evaluated the performance of a compact Pico hydro power plant whose components include an axial hydro turbine, PMG, and power converter. The purpose of the study is to obtain a vast system operating range by passing the generator output voltage between 50–500 V while keeping the THDv consistently below 5%. The simulation results show that at the lower limit of the voltage (50 V), the THDv is 3.63%, while at the upper limit (500 V), it is 2.2%. The power characteristic at the current and frequency variables produces the highest efficiency of around 93% and 87.20% at nominal frequency. From these results, it can be concluded that the proposed system works well as expected.

#### ACKNOWLEDGEMENTS

The authors are grateful to the Excellence Research Program, Bandung Institute of Technology (*Program Riset Unggulan ITB*), for funding this work, and the Research Center for Energy Conversion and Conservation, National Research and Innovation Agency, for the supporting facilities.




#### REFERENCES

- [1] D. Zhou and Z. Deng, "Ultra-low-head hydroelectric technology: a review," *Renew. and Sustain. Ener. Rev.*, vol. 78, pp. 23–30, Oct. 2017, doi: 10.1016/j.rser.2017.04.086.
- [2] I. Safdar, S. Sultana, H. A. Razaa, M. Umerb, and M. Alia, "Empirical analysis of turbine and generator efficiency of a Pico hydro system," *Sustain. Ener. Tech. and Asses.*, vol. 37, pp. 1–7, 2020, doi: 10.1016/j.seta.2019.100605.
- [3] A. Y. Hatata, M. M. El-Saadawi, and S. Saad, "A feasibility study of small hydro power for selected locations in Egypt," *Ener. Stra. Rev.*, vol. 24, pp. 300–313, 2019 doi: 10.1016/j.esr.2019.04.013.




- [4] E. Quaranta and G. Müller, "Sagebien and zuppinger water wheels for very low head hydropower applications," *J Hydr. Res.*, pp. 1–11, 2018, doi: 10.1080/00221686.2017.1397556.
- [5] S. Dhakal *et al.*, "Comparison of cylindrical and conical basins with optimum position of runner: gravitational water vortex power plant," *Renew. and Sustain. Ener. Rev.*, vol. 48, pp. 662–669, 2015, doi: 10.1016/j.rser.2015.04.030.
- [6] Warjito, Budiarsa, A. I. Siswantara, D. Adanta, M. Kamal, and R. Dianofitra, "Simple bucket curvature for designing a low-head turgo turbine for Pico hydro application," *Int. J Tech.*, vol. 7, pp. 1239–1247, 2017, doi: 10.14716/ijtech.v8i7.767.
- [7] E. Gallego, A. R. Clemente, J. Pineda, L. Velásquez, and E. Chica, "Experimental analysis on the performance of a Pico-hydro turgo turbine," *J King Saud Univ. – Eng. Sci.*, vol. 33, pp. 266–275, May 2021, doi: 10.1016/j.jksues.2020.04.011.
- [8] E. Y. Setyawan, Y. I. Nakhoda, A. U. Krismanto, L. Mustiadi, E. Yandri, and J. Burlakovs, "Design and construction of single phase radial flux permanent magnet generators for Pico hydro scale power plants using propeller turbines in water pipes," in *E3S Web of Conf.*, Oct. 2019, pp. 1–10, doi: 10.1051/e3sconf/202018800006.
- [9] S. S. Katre and V. N. Bapat, "Induction generator for Pico-hydro generation as a renewable energy source," in *2015 Int. Conf. on Ener. Syst. and Appl.*, 2015, pp. 130–134, doi: 10.1109/ICESA.2015.7503326.
- [10] S. J. Williamson, A. Griffo, B. H. Stark, and J. D. Booker, "A controller for single-phase parallel inverters in a variable-head Pico-hydropower off-grid network," *Sustain. Ener., Grids and Net.*, vol. 5, pp. 114–124, 2016, doi: 10.1016/j.segan.2015.11.006.
- [11] V. P. Chandran, S. Murshid, and B. Singh, "Improved TOGI based voltage and frequency control for pmsg feeding single-phase loads in isolated Pico-hydro generation," *IETE J Res.*, pp. 1–17, 2019, doi: 10.1080/03772063.2019.1571953.
- [12] V. Leite, J. Couto, Á. Ferreira, and J. Batista, "A practical approach for grid-connected Pico-hydro systems using conventional photovoltaic inverters," in *Proc. IEEE Int. Ener. Conf.*, 2016, pp. 1–6, doi: 10.1109/ENERGYCON.2016.7513911.
- [13] S. Różowicz, Z. Goryca, G. Peczkis, and A. Korczak, "Pico hydro generator as an effective source of renewable energy," *Przełąd Elektr. (Elect. Rev.)*, vol. 1, pp. 202–206, Apr. 2019, doi: 10.15199/48.2019.04.37.
- [14] Z. Liu, H. Liu, W. Wu, W. Shih, and C. Wang, "Development of a standalone Pico-hydropower system in monitoring the gully environment applications in pingtung ur-pho gully," in *Proc. IEEE Eurasia Conf. on IOT, Comm. and Eng.*, Oct. 2019, doi: 10.1109/ECICE47484.2019.8942791.
- [15] P. Kerdtuad, T. Simma, K. Chaiamarit, and S. Visawaphatradhanadhorn, "Establishment of a Pico hydro power plant using permanent magnet synchronous generator supplied for AC microgrid," in *Proc. Int. Elect. Eng. Cong.*, 2018, pp. 1–4, doi: 10.1109/IEECON.2018.8712214.
- [16] G. Subhashini, D. Munandy, and R. Abdulla, "Generating a lighting system by using Pico hydro system," *TELKOMNIKA Telecommunication Computing Electronics and Control*, vol. 15, pp. 1565–1573, Dec. 2017, doi: 10.12928/TELKOMNIKA.v15i4.7235.
- [17] P. Irasari, P. Sutikno, P. Widiyanto, and Q. Maulana, "Performance measurement of a compact generator - hydro turbine system," *Int. J Elect. and Comp. Eng.* vol. 5, pp. 1252–1261, Dec. 2015, doi: 10.11591/ijece.v5i6.pp1252-1261.
- [18] D. Fallows, S. Nuzzo, A. Costabeber, and M. Galea, "Harmonic reduction methods for electrical generation: a review," *IET Gener., Trans. & Distr.*, vol. 12, pp. 3107–3113, May 2018, doi: 10.1049/iet-gtd.2018.0008 .
- [19] I. Sami, N. Ullah, S. M. Muyeen, K. Techato, M. D. S. Chowdhury, and J. Ro, "Control methods for standalone and grid connected micro-hydro power plants with synthetic inertia frequency support: a comprehensive review," *IEEE Access*, vol. 8, pp. 176313–176329, 2020, doi: 10.1109/ACCESS.2020.3026492.
- [20] B. A. Mhlambi, K. Kusakana, and J. Raath, "Voltage and frequency control of isolated Pico-hydro system," in *Proc. Open Innov. Conf.*, Oct. 2018, pp. 246–250, doi: 10.1109/OI.2018.8535603.
- [21] K. Rana and D. C. Meena, "Self excited induction generator for isolated Pico hydro station in remote areas," in *Proc. IEEE Int. Conf. on Power Electr., Intell. Cont. and Ener. Syst.*, 2018, pp. 821–826, doi: 10.1109/ICPEICES.2018.8897329.
- [22] R. Nazir, Syafii, A. Pawawoi, F. Akbar, and A. Dorinza, "Differences in the impact of harmonic distortion due to the installation of electronic load controller in self-excited induction generator and synchronous generator," *Int. J Power Electr. and Drive Syst.*, vol. 10, pp. 104–116, March 2019, doi: 10.11591/ijpeds.v10.i1.pp104-116.
- [23] A. Muis, "Development of blades and cascades of very low head axial flow water turbine (in Bahasa)," Ph.D. dissertation, Fac. Mech. and Aero. Eng., ITB, Bandung, Indonesia, 2016.
- [24] P. Irasari, K. Wirtayasa, P. Widiyanto, M. F. Hikmawan, and M. Kasim, "Characteristics analysis of interior and inset type permanent magnet motors for electric vehicle applications," *J Mechatr., Elect. Power, and Veh. Tech.*, vol. 12, pp. 1–9, 2021, doi: 10.14203/j.mev.2021.v12.1-9.
- [25] Leonics, "Apollo WTC-300 Series". [https://www.leonics.com/product/renewable/inverter/dl/p\\_len\\_bro\\_wtc\\_131.pdf](https://www.leonics.com/product/renewable/inverter/dl/p_len_bro_wtc_131.pdf). (Accessed August 16, 2022).
- [26] A. C. Barmpatza and J. C. Kappatou, "Finite element method investigation and loss estimation of a permanent magnet synchronous generator feeding a non-linear load," *Energies*, vol. 11, 2018, doi: 10.3390/en11123404.
- [27] G. C. Garg and P. S. Bimbhra, *Electrical Machines - I*, 1st ed. India: Khanna Book Publishing Co. (P) Ltd. , 2018.
- [28] M. Satyanarayana and P. S. Kumar, "Analysis and design of solar photo voltaic grid connected inverter," *Indo. J Elect. Eng. and Infor.*, vol. 3, pp. 199–208, Dec. 2015, doi: 10.11591/ijeeci.v3i4.174.

## BIOGRAPHIES OF AUTHORS






**Pudji Irasari**    completed B.Eng. degree in Universitas Brawijaya in 1994 and M.Sc. degree at Oldenburg University, Germany in 2003. Her research interests include analysis of renewable energy power system, electric machine design, and electrical power system assessment. She is currently conducting a low head hydropower systems project at the Research Center for Energy Conversion and Conservation, The National Research and Innovation Agency (BRIN), Indonesia. She can be contacted at email: pudj003@brin.go.id, or pirasari@yahoo.com.






**Anwar Muqorobin**    was born in Temanggung, Indonesia in 1977. He received the bachelor degree from Universitas Diponegoro in 2001, the master degree from Institut Teknologi Bandung in 2013, and the doctoral degree from Institut Teknologi Bandung in 2019, all in Electrical Engineering. He is currently a researcher at Research Center for Energy Conversion and Conservation, National Research and Innovation Agency (BRIN). His research interest is inverter. He can be contacted at email: [anwa006@lipi.go.id](mailto:anwa006@lipi.go.id), or [anwa006@gmail.com](mailto:anwa006@gmail.com).






**Puji Widiyanto**    received his B. Eng. and M. Eng. degrees both in Mechanical Engineering, first in STT Mandala and later in Institute Technology Bandung. Having focused his research on the structure and mechanical design of electrical machines, he is now working as a researcher at the Research Center for Energy Conversion and Conservation, The National Research and Innovation Agency (BRIN). Currently, he is conducting a project on low head hydropower system. He can be contacted at email: [puji010@brin.go.id](mailto:puji010@brin.go.id), or [pujiwidiyanto@gmail.com](mailto:pujiwidiyanto@gmail.com).






**Tajuddin Nur**    received his B.E. from Department of Electrical Engineering (power system and electrical machine) from Hasanuddin University Makassar, South Sulawesi (Indonesia), M.Eng degree in electrical engineering (electrical machine) from Indonesia University (UI) Depok, West Java Indonesia. He got his Ph.D (in electrical machine analysis) at Department of Electrical Engineering, Graduate School of Engineering, Southern Taiwan University (STUT), Taiwan. His current research interest in electrical machine analysis, renewable energy, power generation, power quality, finite element and power electronics. Dr. Tajuddin is a frequent reviewer of International Conference on Electric Machines and Systems (ICEMS). He can be contacted at email: [tajuddinnur559@gmail.com](mailto:tajuddinnur559@gmail.com).



**I Nengah Diasta**    is a researcher at the Research Center for New and Renewable Energy, Institut Teknologi Bandung, Indonesia since 1994. He received the bachelor degree (1991) and master degree (1997) from Institut Teknologi Bandung, Indonesia. His research focuses on the area of fluid mechanics and fluid machineries. He can be contacted at email: [inengahdiasta@itb.ac.id](mailto:inengahdiasta@itb.ac.id), or [inengahdiasta@gmail.com](mailto:inengahdiasta@gmail.com).



**Priyono Sutikno**    completed his bachelor degree in Mechanical Engineering, Bandung Institute of Technology (ITB), in 1976. He continued his master study in Automatic Control ENSM in 1981 and received his Diplome de Docteur Ingenieur in 1984 from the University of de Perpignan, France. His research interest and competence include Fluid Mechanic, Turbomachinery, and CFD. Currently he is a Professor at the Laboratory of Fluid Machinery, ITB. He can be contacted at email: [priyono@itb.ac.id](mailto:priyono@itb.ac.id), [priyonosutikno@gmail.com](mailto:priyonosutikno@gmail.com), or [priyono@ftmd.itb.ac.id](mailto:priyono@ftmd.itb.ac.id).